 doi:10.20944/preprints201805.0007.v1

Article

Climate change impacts assessment in coastal lagoons using available modelling tools

Bruno Primo [1,2]*, Fernanda Achete[1,2], Sarith Mahanama[3], Marcus Thatcher[4], Mark Hemer[5], Sutat Weesakul[6] and Trang Duong[7]

[1] Universidade Federal do Rio de Janeiro (UFRJ), Rio de Janeiro, RJ, Brazil
[2] Vortex Mundus, Rio de Janeiro, RJ, Brazil
[3] Global Modeling and Assimilation Office, NASA, Goddard Space Flight Center, Greenbelt, Maryland, USA
[4] CSIRO Oceans & Atmosphere, Private Bag 1, Aspendale VIC 3195, Australia
[5] CSIRO Oceans & Atmosphere, GPO Box 1538, Hobart TAS 7001 Australia
[6] Asian Institute of Technology, Bangkok, Thailand, Hydro and Agro Informatics Institute, Bangkok, Thailand
[7] IHE Delft and Deltares
* Correspondence: brunovps@gmail.com; Tel.: +55-21-98828-0606

Abstract: Climate change such as sea level rise, change in temperature, precipitation, and storminess are expected to impact significantly coastal lagoons. The nature and magnitude of these impacts are uncertain. The objective of the research is to determine the climate change impacts on mixing and circulation at Songkhla lagoon, Thailand. Songkhla lagoon is the largest lagoonal water resource in Thailand and Southeast Asia. The lagoon is a combined freshwater and estuarine complex of high productivity which represents an extraordinary combination of environmental resources believed to be unique in the region.

This work is part of a Climate Change impact assessment framework. It is the validation phase (step 5) of the framework applying a case study. Delft 3D was used to simulate CC scenarios in the climate downscaling models, part of the previous framework steps. These results were compared to the current conditions to determine the main changes in mixing and circulation in the coastal lagoon. Three indicators were applied to quantify the impacts: flushing time, salinity intrusion and stratification.

The results suggest an increase in water velocities at the inlet in future scenarios and a decrease of flushing time. Salinity and stratification showed more complex changes in futures scenarios.

Keywords: water quality; hydrodynamics; flushing time; residence time; downscaling; stratification

1. Introduction

A coastal lagoon is a shallow water body separated from the ocean by a barrier, connected at least intermittently to the ocean by one or more restricted inlets [1,2]. They account for thirteen percent of all coastal environments and usually are poorly flushed and exhibit long resident times [3,4]. Coastal lagoons support a range of natural services that are highly valued by society, including but not limited to fisheries, storm protection, and tourism. They are highly productive ecosystems and support a variety of habitats including salt marshes, seagrasses, and mangroves. They also provide essential habitat for many fish and shellfish species [5].

 doi:10.20944/preprints201805.0007.v1

Coastal lagoons are ephemeral on a geologic time scale and were formed by a combination of sea-level variation and longshore drift [2,5]. Near the end of Pleistocene (15,000 years ago), the mean sea level rose 130m flooding river valleys and low-lying coastal depressions. Sediment transport can reshape the coast by growing spits and barriers islands forming coastal lagoons [6]. These lagoons can also be formed in marginal depressions behind barriers of active river delta systems [7]. Once formed, they are subject to rapid sedimentation and will eventually change into other types of environments through sediment infilling, tectonic activity, eustatic change in sea level, and land-use activities. Geologically, this change is rapid and can be expected to occur within decades to centuries [6].

The size of coastal lagoons varies substantially, ranging in area from less than 0.01km^2 to more than 10,000 km^2, as in the case of Lagoa dos Patos – Brazil. The average depth varies from 1 to 3 m and rarely is exceed 5m, except for the inlet and other tidal channels. Depending on local climatic conditions, salinity can vary from completely fresh to hypersaline [2].

Coastal lagoons experience the same forcing as coastal estuaries: river inflow, wind stress, tides, precipitation-evaporation balance, and surface heat balance. However, they respond unequally to these forcing because of differences in geomorphology. The lagoon circulation determines the water and salt balance, water quality, eutrophication, turnover, residence and flushing times [2]. Hydrodynamics and water renovation are of prime importance for planning and implementation of coastal management strategies in coastal lagoons [6]. Although circulation, mixing and exchange have been studied extensively in coastal plain estuaries, these processes have been less synthesized for coastal lagoons.

1.1 CC impacts on coastal lagoons

Climate change is expected to impact sea level rise (SLR), temperature, precipitation, and storminess; therefore, severe changes are expected to occur in coastal lagoons [5,8]. In this study the impacts of sea level rise and precipitation were investigated.

1.1.1 Sea Level Rise (SLR)

Due to glacial melting and thermal expansion of the oceans, mean sea level, on a global scale, has been increasing over the past century and is expected to keep increasing in the future. IPCC (2007) estimated an increase between 0.18 and 0.79 (including an allowance of 0.2m for the uncertainty related to Ice sheet flow) by the end of 21st century.

The rapid change in sea level can profoundly alter estuarine ecosystem worldwide. The most affected are the low-lying estuaries where the higher sea levels increase the salt water exchange rate increasing salinity inside the estuary. Higher salt concentration impacts the system ecology as well as circulation due to baroclinic processes [8].

SLR leads to increase of overall estuarine depth. Light attenuation is directly proportional to local depth, therefore deeper estuaries decrease primary production and impacting the entire food web. It increases the chances of anoxic sediment changing geochemical processes and enhance stratification, since it requires higher wind stresses to mix the deeper water column [8,5].

1.1.2 Precipitation

Global Climate Change will modify the precipitation regime intensity, timing, volume and distribution. Superficial runoff is dependent on the precipitation and soil cover, so the increase in precipitation may increase delivery of nutrients. At the same time the changes in runoff can impact the lagoon flushing time.

Change in precipitation affects salinity in estuaries, the increase of freshwater runoff decrease salinity on contrary the decrease in precipitation increase estuarine salinity. Modification in salinity impacts the estuary stratification which may lead to hypoxia in the deeper regions [5].

Preprints (www.preprints.org) | NOT PEER-REVIEWED | Posted: 1 May 2018 doi:10.20944/preprints201805.0007.v1

1.2 *Climate Change Impact Assessment Framework*

Numerical models are widely applied tool to investigate the possible impacts of the aforementioned forcing changes would have on coastal lagoon. Climate change impacts investigation would require a simulation for the entire period of interest, typically 50-100 years. However, simulations for more than 5 years, even with reduced and schematized forcing conditions have been unsuccessful [9]. A number of studies have been attempted using different approaches to perform long period simulations [10-13] but have been only partially successful. The main problem of these approaches is the accumulation of numerical errors in the computational domain.

A model capable of producing reliable 50-100 year predictions with concurrent water level, wave and river flow forcing does not currently exist. Even if such model was available, the high computational demand of the model would limit the number of scenarios and reduce the capacity to simulate the large uncertainty inherent to climate change impact studies. Climate change impact assessment contain many uncertainties. In order to reduce these uncertainties, a train of numerical models could be used. [14] present an ensemble modeling framework that could be used for robust assessment climate change impacts (Figure 1). This approach shows the model development from a global scale to a local site scale via a logical sequencing. The last step (Step 5) of the approach is related to the use of an appropriate coastal impact model for investigating the system diagnostic.

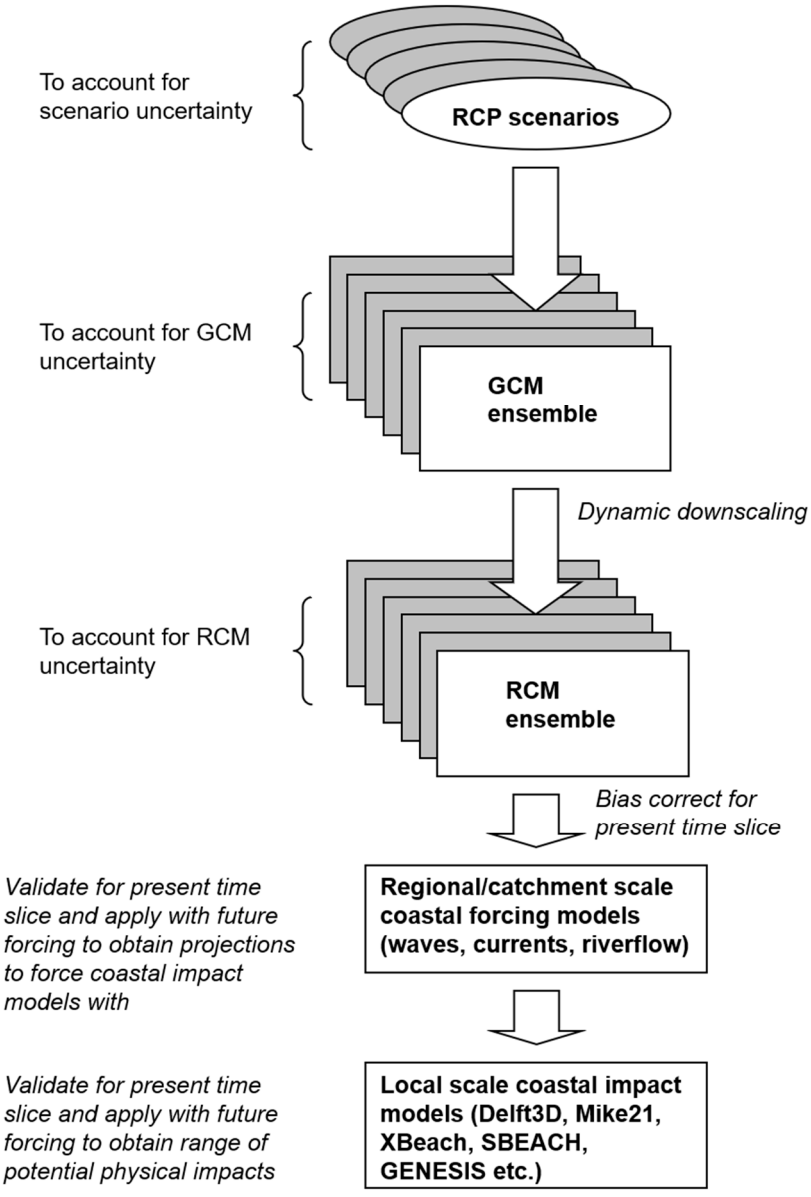

Preprints (www.preprints.org) | NOT PEER-REVIEWED | Posted: 1 May 2018 doi:10.20944/preprints201805.0007.v1

Figure 1: Suggested standard modelling framework for a climate change impact quantification study on sandy coasts [from: 15].

This work is embedded in this framework as an application of step 5. The aim of this paper is to measure the potential impact of CC in mixing and circulation of coastal lagoons using three different indicators flushing time, salinity and stratification. Songkhla lagoon, Thailand is used as study case. This study is part of a project called "Climate Change Impacts on Small Tidal Inlets (CC-STI)" lead by UNESCO-IHE. The main objective of CC-STI is to determine how the climate change will impact on STIs and what are the best adaptation strategies.

We perform short simulations considering future climate change scenarios, derived from the previous framework steps. A process-based model is calibrated and validated for the present conditions then simulated for a period of one year using possible future forcing (e.g. 2050, 2100).

2. Materials and Methods

In this session we briefly describe the models and steps followed to apply the CC assessment framework until the step 5, the focus of this work.

2.1 CC framework Model Description

2.1.1 Atmospheric Model

The atmospheric model used as step 1 in this study was the Conformal Cubic Atmospheric Model (CCAM). The CCAM is designed as a semi-implicit, semi-Lagrangian atmospheric climate model based on a conformal cubic grid [16,17]. A variable resolution grid was used by applying Schmidt transformation [18], which results in a finer grid resolution over the target area at the expense of a coarser resolution on the opposite side of the globe (Figure 2).

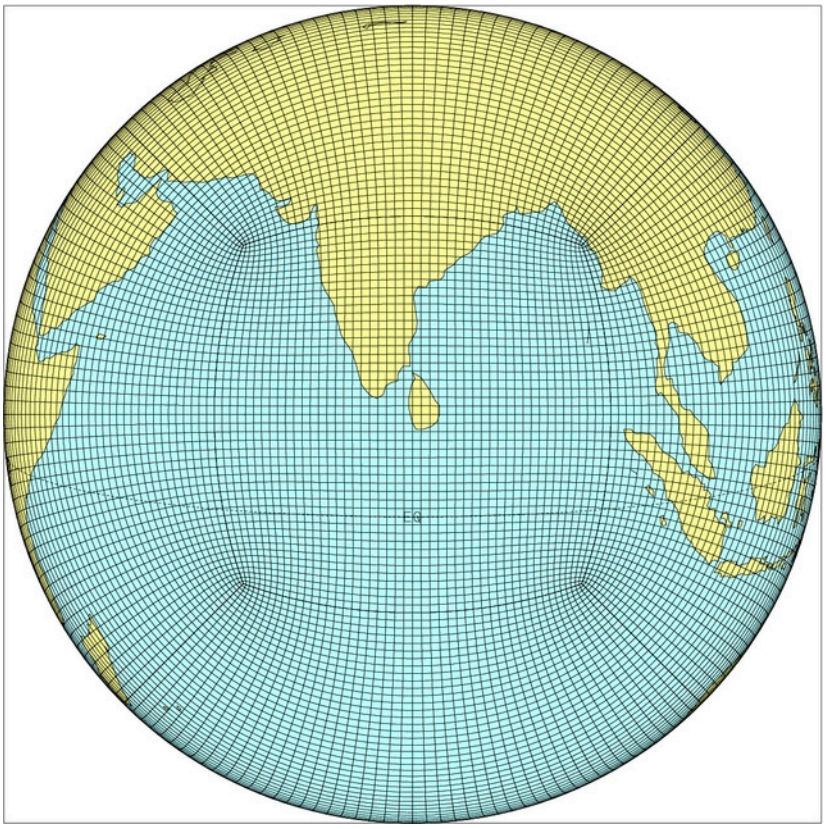

Figure 2: Plot of the variable resolution conformal cubic grid used for the finer resolution simulations discussed in this paper.

 doi:10.20944/preprints201805.0007.v1

The CCAM physical parameterizations used for this paper include a prognostic cloud scheme [19] and convection based on the approach by [20]. The land-surface scheme supports 6 levels of soil temperature and moisture as well as up to three levels of snow [21]. For these experiments a stability dependent boundary layer scheme was used [22] with non-local vertical mixing following [23], and enhanced mixing of cloudy boundary layer air [24]. Gravity wave drag is parameterized following [25]. Short wave and Long wave radiation for these experiments was parameterized according to [26,27], respectively. Eighteen vertical levels were from 40m to 35km.

Step 2 accounts for uncertainty, Sea Surface Temperatures are taken from six CMIP3 General Circulation Models (GCMs) to provide a surface boundary condition for ocean grid points. Monthly biases in the GCM SST datasets were estimated from the 20C3M experiment (1971-2000) after comparing with Reynolds SST climatology. The monthly biases where then subtracted from the GCM SSTs for each simulation month, including the future climate. This provided a 'bias corrected' SST dataset. Once the bias corrected GCM SST datasets are generated, CCAM is run without atmospheric nudging to create an atmospheric dataset which is consistent with the changes to the SSTs.

Two of the better performing 65 km resolution host simulations (i.e., SSTs from GFDL2.1 and ECHAM5 GCMs) were selected to further downscale to approximately 15 km resolution over Thailand, step 3. The 15 km resolution experiments used a C48 grid (i.e., 48 x 48 grid points in the horizontal for each of the six cubic panels). To compensate for errors arising from the coarse resolution region on the opposite side of the globe to the target region, we use a scale-selective filter [28], which perturbs the simulated atmosphere towards the host 65 km resolution simulation at length scales greater than 700 km in diameter. In this way, large scale atmospheric circulation is assimilated from the host 65 km resolution simulation, whereas finer scale atmospheric behavior is simulated by the nested simulation. This approach ensures a high degree of consistency between the host and regional model.

2.1.2 Hydrological Model

In step 4, the hydrologic model used in this study is the Catchment Land Surface Model (CLSM: [29,30]). CLSM is a macroscale hydrologic model that balances both surface water and energy at the Earth's land surface. The controls of vegetation on land–atmosphere moisture and energy fluxes within CLSM can be considered to constitute a soil–vegetation–atmosphere transfer scheme (SVAT). One distinguishing characteristic of CLSM is that it considers irregularly shaped, topographically delineated, hydrologic catchment as the fundamental element on the land surface for computing land surface processes. Each catchment is further partitioned into three regimes: 1) a saturated region, from which evaporation occurs with no water stress and over which rainfall is immediately converted to surface runoff, 2) a sub-saturated region, from which transpiration occurs with no water stress and over which rainwater infiltrates the soil, and 3) a ''wilting'' region, in which transpiration is shut off. The relative areas of these regions vary dynamically; they are unique functions of the Catchment LSM's three water prognostic variables and the topographic characteristics of the catchment. By continually partitioning the catchment into hydrologically distinct regimes and then applying different regime-appropriate physics within each regime, the Catchment LSM should, at least in principle, provide a more realistic representation of surface energy and water processes. Thus, in contrast with most SVATs, the CLSM accounts for the spatial heterogeneity in soil moisture characteristics within computational elements. In Sri Lanka the model reproduced observed streamflow with a greater degree of accuracy and they extended their study to investigate the impact of soil moisture initial conditions to seasonal streamflow predictability [31].

2.1.3 Meteorological Forcing

A suite of widely used Atmosphere Ocean General Circulation Models (AOGCMs) produced climate simulations for various carbon dioxide emission scenarios for the Intergovernmental Panel on Climate Change Fourth Assessment Report (IPCC AR4). Climate simulations from two AOGCMs (ECHAM and GFDL) for the Special report on Emission Scenario (SRES) A2 were chosen for the

 doi:10.20944/preprints201805.0007.v1

climate change impact analyses. SRES A2 is characterized by heterogeneous world with increasing global population and regional economic growth. The CSIRO CCAM Regional Climate Model dynamically downscaled ECHAM and GFDL climate simulations and provided surface meteorological forcings for the study. The provided 6-hourly, 0.5-degree, surface meteorological forcings included shortwave radiation, longwave radiation, total precipitation, convective precipitation, surface pressure, air temperature at 2m, specific humidity at 2m, and wind for 3 different periods: i) hindcast, climate simulations for the period 1981-2000; ii) climate projections for the period 2041-2060, and iii) climate projections for the period 2081-2100. The Catchment Land Surface Model was forced in offline mode using downscaled surface meteorological forcings to generate streamflow at river mouths in study lagoons.

2.1.3 Coastal Model

The step 5 is the validation of the framework in a local scale. The coastal model used for this step was Delft3D. Delft3D-FLOW is a multi-dimensional (2D or 3D) hydrodynamic and transport modeling system of Deltares for the aquatic environment which calculates non-steady flow and transport phenomena that result from tidal and meteorological forcing on a rectilinear or a curvilinear, boundary fitted grid [32]. The differential equations solved numerically in the model are: the horizontal momentum equations, the continuity equation, the transport equation, and a turbulence closure model. Vertical accelerations are assumed to be small so the vertical momentum equation is reduced to the hydrostatic pressure relation. In 3D simulations, the vertical grid is defined following the sigma co-ordinate approach.

Delft3D-WAQ is a 3-dimensional water quality model that solves the advection-diffusion-reaction equation and allows great flexibility in the substances to be modeled. It should be coupled to Delft3D-FLOW or another model to get hydrodynamic conditions.

2.2 Study Area

Songkhla lagoon is the largest lagoonal water resource in Thailand and Southeast Asia and is made up of three interconnected lakes (Figure 3). Southern Songkhla Lake, known as Thale Sap Songkhla, is the outer lagoon of the system and discharges into the Gulf of Thailand through a small channel which also serves as the harbor entrance to the town of Songkhla. The depth of the harbor and its channel are maintained at six to eight meters. An open lagoon with an undisturbed circulation of fresh and brackish water is a prerequisite for a stable and healthy ecosystem. Any change in this dynamic, whether from natural or man-induced actions, is likely to affect the whole system.

Preprints (www.preprints.org) | NOT PEER-REVIEWED | Posted: 1 May 2018 doi:10.20944/preprints201805.0007.v1

213

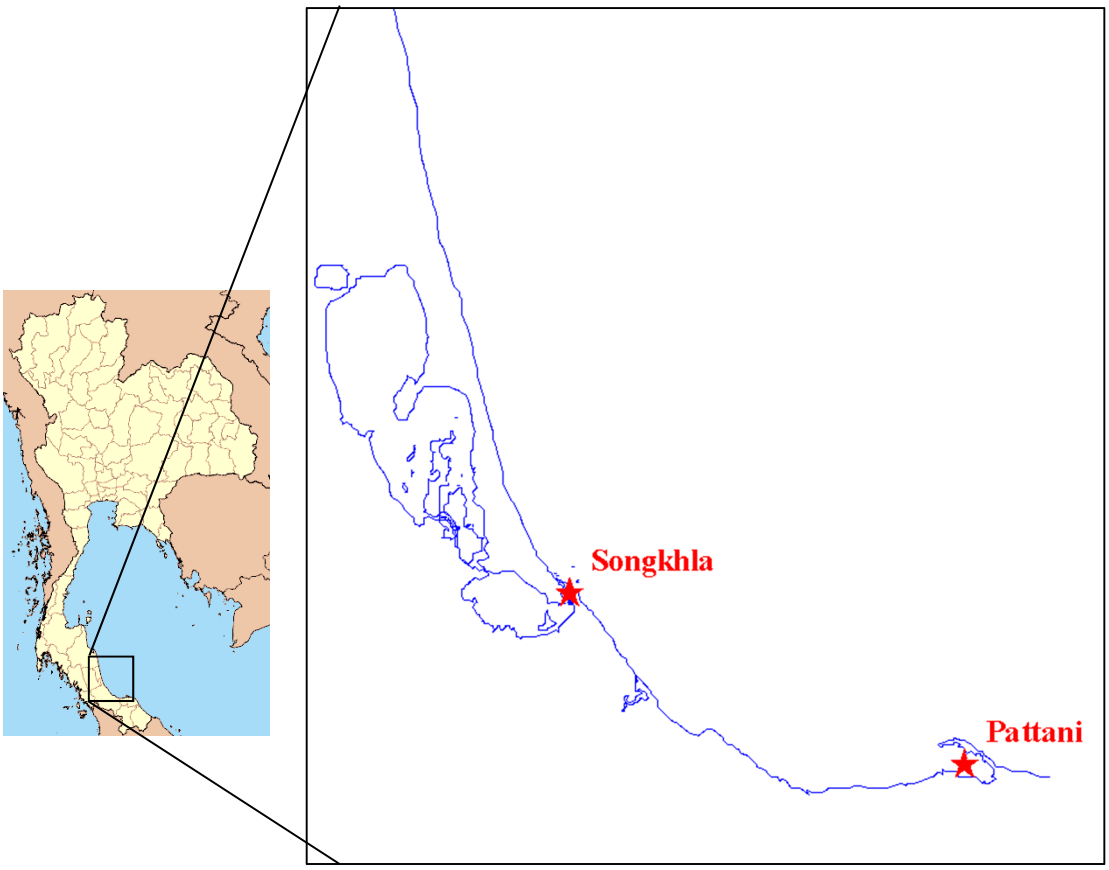

214

215 Figure 3: Location Map of Songkhla Lagoon

216 Around 21 years of hourly water level data is available for two points: Songkhla and Pattani.
217 These data were used as calibration of the numerical model. The maximum tidal range is about 0.7m
218 for Pattani and 0.6 for Songkhla during spring tides
219 Velocity data was digitalized from [33]. Current measurements of two points were conducted
220 during the dry season during 6 days of 1997. The points are located in the two channels formed by
221 the island, one at the north and one at the south of the Ko Yo island. The observed tidal current
222 fluctuation north of Ko Yo Island in June 1997, shows a maximum current speed of about 0.4 m/s
223 during flood tide (Figure 6). South of Ko Yo the maximum registered was about 0.3 m/s.
224 Salinity data was digitalized from [34]. The point is located very close to the island in a very
225 shallow area and the measurement was conducted during October of 2006.The observed salinity
226 fluctuation at point A, shows a maximum salinity of about 32.4 psu and a minimum of about 31.
227 The curvilinear model grid was constructed in a spherical coordinate system with the total of
228 10159 grid cells using the Delft3D-RGFGRID. The grid size varies in space such that finer grids are
229 located in the inlet (20x30 m) and coarser (370x420 m) grids are located in the northern part of the
230 lake (Figure 4) 10 vertical layers were used.
231 The bathymetry inside the lagoon has an average depth of 1.5m. Most of the lagoon has a depth
232 around 2m, in the channel entrance the depth is around 8m. This channel divides into two near the
233 island; the north part has a depth greater than the south part. Pak Ro, the channel which connects
234 Thale Luang with Thale Sap Songkhla is also relatively deep. Outside the lagoon, 7km from the
235 entrance channel, the depth reaches 13m.

236 2.2.1 Initial and boundary conditions

237 In this study, two types of open boundaries were used: Water level and Total discharge. Water
238 level was used in the ocean boundary (northeast of the domain). World Tides astronomic components

Preprints (www.preprints.org) | NOT PEER-REVIEWED | Posted: 1 May 2018 doi:10.20944/preprints201805.0007.v1

with its respective corrections were used to force this boundary. World Tides is a general-purpose program for the analysis and prediction of tides. Using least squares harmonic analysis, it allows the user to decompose a water level record into its tidal and non-tidal components by fitting between 5 and 35 user-selectable tidal frequencies (tidal harmonic constituents).

River discharge was used in the other two open boundaries where the rivers of the domain are present, time series of river discharge were used in these cases. The boundary in the south part of the lagoon represents the river Khlong Utaphao, while the one in the western part represents the river Khlong Rattaphum (Figure 4).

Sensitivity analysis in time step, viscosity and eddy diffusivity was done. The optimum time step for the chosen grid was 30 second. The appropriate eddy viscosity found was 0.1m2/s and eddy diffusivity of 0.05 $m^2 s^{-1}$.

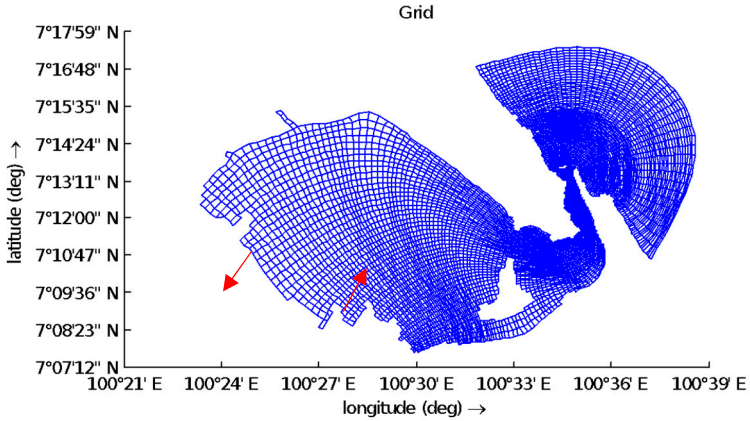

Figure 4: Songkhla Lagoon coastal model grid, red arrows represent the rivers Khlong Utaphao and Rattaphum.

The bathymetry inside the lagoon has an average depth of 1.5m. Most of the lagoon has a depth around 2m, in the channel entrance the depth is around 8m. This channel divides into two near the island; the north part has a depth greater than the south part. Pak Ro, the channel which connects Thale Luang with Thale Sap Songkhla is also relatively deep. Outside the lagoon, 7km from the entrance channel, the depth reaches 13m.

2.3. Flushing time

Delft-WAQ model was used to calculate the flushing time. The transport and dispersion of a conservative tracer inside the lagoon and its exchange with the ocean is examined. A uniform concentration of 1mg/l is set inside the lagoon, while a concentration of 0mg/l is set at the ocean boundary condition. Hydrodynamic results of simulations with different conditions of river flow and sea level as defined earlier was coupled with this model. The concentrations averaged for the entire lagoon for each time step is calculated to investigate flushing of the lagoon. This signal is filtered to eliminate high frequencies due to tide oscillations.

The percentage of the initial mass of the tracer remaining within the lagoon was calculated at each time step and was expressed as an exponential curve of the following form to obtain the e-folding time (the time taken for the initial mass to reduce to 1/e of initial mass) for the lagoon.

$$Y = Aexp(bT), \quad (1)$$

Where, Y = Percentage mass remaining, T = Time in hours, A, b = constants. The e-folding time is an estimate the flushing time of the lagoon [35].

Preprints (www.preprints.org) | NOT PEER-REVIEWED | Posted: 1 May 2018 doi:10.20944/preprints201805.0007.v1

3. Results

3.1. Hydrodynamic Model

In order to guarantee the reliability, the model should be calibrated against hydrodynamic measurements, such as water level and velocity. To calibrate the model for water level, the available water level data for Songkhla was used (Figure 5). The model results agree with the data in amplitude and phase.

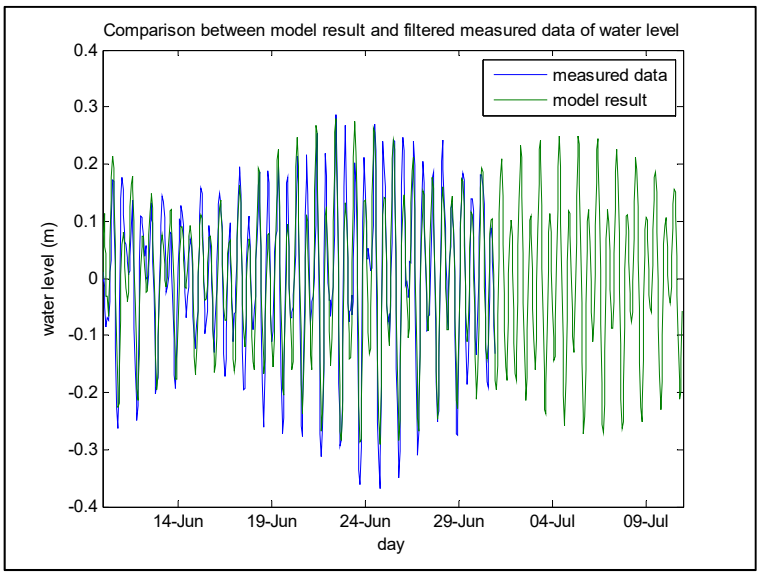

Figure 5: Comparison between model result and filtered measured data of Songkhla water level during July 1997.

Velocity calibration was done using velocity data at two different locations: North and South of Ko Yo Island. The comparison between data and model results for the two points are plotted in Figure 6. The results from North of Koyo show a phase lag of 2 hours comparing to the data, but the amplitude of the tidal currents is well correlated. The South of Koyo results show smaller amplitude when compared to the data, but the difference is very small, less than 0.05 m/s. Despite these small differences, the model was considered well calibrated.

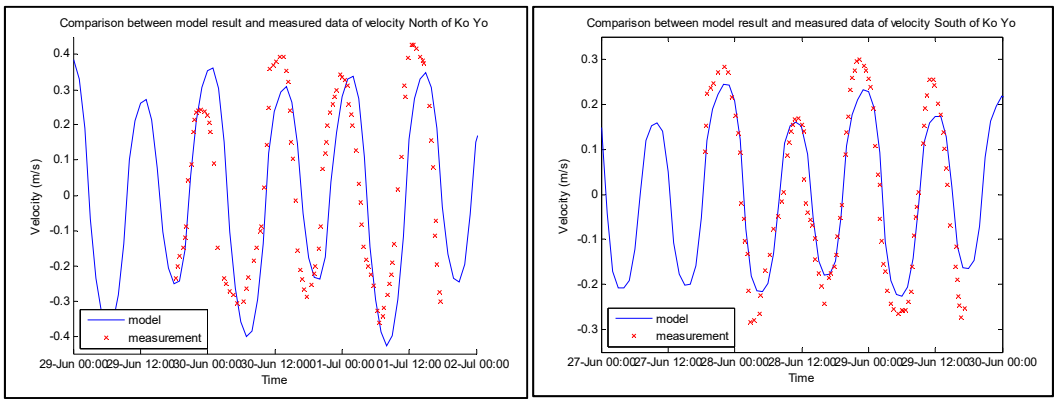

(a) (b)

Figure 6: Comparison between model results and measured data of velocity at a) North of Ko Yo and b) South Ko Yo.

Preprints (www.preprints.org) | NOT PEER-REVIEWED | Posted: 1 May 2018 doi:10.20944/preprints201805.0007.v1

4. Discussion

After calibration, several scenarios were defined to simulate current and future conditions. For each scenario, a period of 15 days was simulated using Delft3D-Flow and Delft3D-WAQ. The scenarios are summarized in Table 1 and Table 2. To represent the river flows, two models were used: GFDL and ECHAM. These models give the current and future conditions, represented by the year 2000 and 2100 respectively. The dry month is represented by February, while the wet is October. Because the uncertainty about the river flows, two different percentages of the flow given by the two models were used: 5% and 20%.

To represent the sea level rise for the year 2100, the bathymetry for the entire region was deepened by 0.79m, which represents the worst-case estimate of IPCC for the year 2100.

Table 1 – Simulated scenarios input with 5% of the rivers flows

Model	**GFDL**				**ECHAM**			
Year	2000		2100		2000		2100	
Season	wet	dry	wet	dry	wet	dry	wet	dry
Total Flow	5	0.4	4.6	0.065	6.1	0.15	6.7	0.32
Utaphao	4	0.32	3.68	0.052	4.88	0.12	5.36	0.256
Rattaphum	1	0.08	0.92	0.0057	1.22	0.03	1.34	0.064

Table 2 - Simulated scenarios input with 20% of the rivers flows

Model	**GFDL**				**ECHAM**			
Year	2000		2100		2000		2100	
Season	wet	dry	wet	dry	wet	dry	wet	dry
Total Flow	20	2	18.4	0.26	24.4	0.6	26.8	1.3
Utaphao	16	1.28	14.72	0.208	19.52	0.48	21.44	1.04
Rattaphum	4	0.32	3.68	0.052	4.88	0.12	5.36	0.26

The maximum velocities at the inlet are represented in Table 3 and Table 4 According to the results, there are no significant changes of velocities at the inlet between the dry and wet months or between scenarios with 5% and 20% of river flow, which means that probably the river discharges doesn't have high influence on velocities at the inlet. Comparing the current and future scenarios, it can be observed that the maximum velocities in the future will be higher than today due to sea level rise, this increase corresponds to around 20% for all cases. However, it is likely that the inlet morphology will also change in the future in order to preserve inlet equilibrium velocities of around 1 ms-1.

Table 3 - Maximum velocities at the inlet for the scenarios with 5% of river flow

	GFDL				**ECHAM**			
	2000		2100		2000		2100	
Season	wet	dry	wet	dry	wet	dry	wet	dry
Maximum velocity (inlet)	1.05	1.02	1.24	1.25	1.06	1.02	1.24	1.25

Table 4 - Maximum velocities at the inlet for the scenarios with 20% of river flow

	GFDL				**ECHAM**			
	2000		2100		2000		2100	
Season	wet	dry	wet	dry	wet	dry	wet	dry
Maximum velocity (inlet)	1.04	1.03	1.22	1.25	1.06	1.03	1.23	1.25

Preprints (www.preprints.org) | NOT PEER-REVIEWED | Posted: 1 May 2018 doi:10.20944/preprints201805.0007.v1

4.1 Flushing Time

The flushing time results are summarized in Table 5 and Table 6. The results show that for all cases, the flushing time for wet months is smaller than for dry months (22% for 5% of river flow and 111% for the 20% of river flow). Scenarios with 20% of river flow also showed smaller flushing times comparing with the 5% ones. The rivers help to flush the lagoon so its flow is inversely proportional to flushing time. Also, the flushing time will decrease in future scenarios of sea level rise; this decrease will be different, depending on the river flow changes. When the river flow increase, which is the case of ECHAM model, the flushing time have a higher decrease.

Table 5 - Calculated flushing time for the scenarios with 5% of river flow

	GFDL				**ECHAM**			
	2000		2100		2000		2100	
Season	wet	dry	wet	dry	wet	dry	wet	dry
Flushing time (h)	270.05	319.15	199.87	267.36	318.92	331.02	200.70	267.38

Table 6 - Calculated flushing time for the scenarios with 20% of river flow

	GFDL				**ECHAM**			
	2000		2100		2000		2100	
Season	wet	dry	wet	dry	wet	dry	wet	dry
Flushing time (h)	146.6	281.8	110.4	235.9	134.5	281.2	102.7	236.1

4.2 Salinity

All the simulations showed a similar salinity distribution, with different magnitudes Figure 7 shows the result of depth average salinity of the entire lagoon for the scenarios using ECHAM model for the instant 13th October 2000 at 22:00h. This result shows a salinity of 35 psu outside the lagoon. Inside the lagoon the salinity decreases near the rivers, with a minimum of 25 psu close to the river mouth.

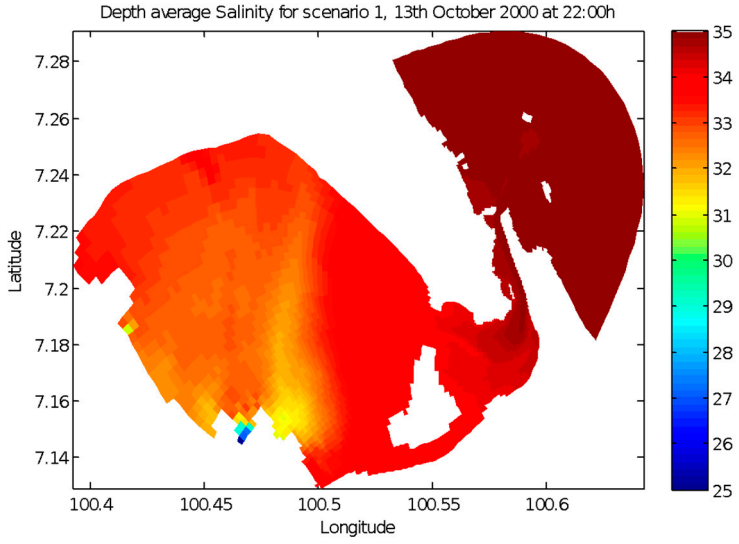

Figure 7: Result for depth average salinity for Scenario ECHAM - 2000 - wet for the instant 13th October 2000 at 22:00h

The mean salinity for a point in the center of the lagoon was calculated and the results are summarized in Table 7 and Table 8. For both models, the results showed a difference in salinities between wet and dry months. The wet months presents lower salinity than the dry months for all the simulations, but especially for the scenarios with 20% of river flow, where the difference can reach

Preprints (www.preprints.org) | NOT PEER-REVIEWED | Posted: 1 May 2018 doi:10.20944/preprints201805.0007.v1

more than 15 psu. The salinity during the dry months didn't show much change for all the scenarios. However, it should be noted that CC driven variation in evaporation was not considered in these simulations.

Table 7 - Mean salinity at a point in center of the lagoon for the different scenarios with 5% river flow

	GFDL				ECHAM			
	2000		2100		2000		2100	
Season	wet	dry	wet	dry	wet	dry	wet	dry
Salinity (psu)	31.52	34	31.44	34	33.24	34	31.13	34

Table 8 - Mean salinity at a point in center of the lagoon for the different scenarios with 20% river flow

	GFDL				ECHAM			
	2000		2100		2000		2100	
Season	wet	dry	wet	dry	wet	dry	wet	dry
Salinity (psu)	15.8	33.0	17.14	33.0	13.05	33.0	14.3	32.9

4.3. Stratification

The stratification of the lagoon is defined as the difference between the bottom and the top layers of the simulation results. Figure 8 shows this difference for the entire lagoon for the scenarios using river flow derived from the ECHAM model for the instant 13th October 2000 at 22:00h. It can be observed that there is no stratification in the east part of the lagoon. The greatest stratification is found on the western part, especially close to the river mouths, where it can reach 15 psu.

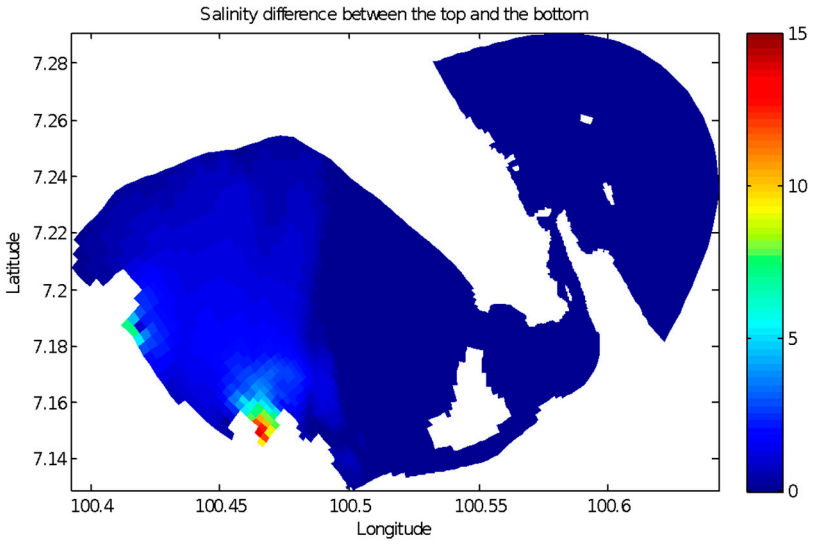

Figure 8: Difference between the bottom and the top layer of salinity results for Scenario ECHAM - 2000 - wet for the instant 13th October 2000 at 22:00h

The maximum stratification for a point located in the west part of the lagoon was calculated and the results are summarized in Table 9 and Table 10. This point was chosen because is a point with significant stratification and not very close to the rivers mouths. The results show that the stratification for this point is greater during wet season. Comparing current with future scenarios, during wet months stratification decreases in the future for the simulations with 5% of river flow and it increases in the simulations with 20% of river flow. For the dry months, all simulations showed an increase in stratification in future. It should be noted that CC driven variations in wind were not considered in these simulations.

Preprints (www.preprints.org) | NOT PEER-REVIEWED | Posted: 1 May 2018 doi:10.20944/preprints201805.0007.v1

Table 9 – Average Difference salinity at a point in the western part of the lagoon for the different scenarios with 5% of river flow

	GFDL				ECHAM			
	2000		2100		2000		2100	
Season	wet	dry	wet	dry	wet	dry	wet	dry
Difference (psu)	1.45	0.33	1.09	0.83	1.72	0.29	1.27	0.81

Table 10 - Average Difference salinity at a point in the western part of the lagoon for the different scenarios with 20% of river flow

	GFDL				ECHAM			
	2000		2100		2000		2100	
Season	wet	dry	wet	dry	wet	dry	wet	dry
Difference (psu)	2.17	0.73	2.30	0.82	2.15	0.36	2.92	0.68

5. Conclusions

The proposed framework is a useful tool to assess Climate Change impacts. The five steps provide a comprehensive analysis from atmospheric modeling, climatic downscaling to impacts in coastal lagoons. The river flow obtained using dynamically downscaled projections from two global models GFDL and ECHAM showed different results. The year of 2000, both showed the same behavior, but different magnitudes. For the year 2100 they showed opposite behavior, ECHAM predicts an increase of river flow, while GFDL predicts a decrease. The high variability associated to the river flow and uncertainties of long prediction are possible reasons for this difference.

Some scenarios were designed to simulate current and future scenarios for the region during dry and wet seasons and for river flow of 5% and 20% of the two available models, with a total of 16 simulations. The results show that circulation in Thale Sap Songkhla is strongly influenced by the lake geometry. The strong flow, coming from the lake entrance, deflects to the north and the south of Ko Yo. The velocities at the entrance channel are around 1m/s and the simulations show an increase of 20% for the year 2100 (in the absence of morphological adjustments, which were not simulated here).

Flushing time, salinity intrusion and stratification, are useful indicators to quantify the impacts of CC in coastal lagoons. For the specific case of Songkhla Lagoon, the flushing time is smaller during wet months, because of the higher river flows and is expected to decrease for future scenarios due to the sea level rise. Salinity has different values for wet and dry months, being higher during dry months because the weaker river flows. Stratification results showed a higher stratification during wet season. The results suggest distinct behavior for future scenarios, during wet months the stratification can decrease or increase depending on river flow considerations. During dry months, it will increase for future scenarios. This result was not sufficient and further analysis should be done to find the reasons for this behavior.

For future modeling efforts, there is an urgent need for high quality simultaneous measurements of water level, velocity, and salinity at several points spread across the lagoon over a duration of at least 30 days during both the wet and dry seasons. River discharge data and atmospheric data, such as: wind, evaporation, rainfall, solar incidence should also be measured.

The main limitation of this study is the lack of data for the region. Due to this limitation, the results of this study should be interpreted in a qualitative way. The comparison between the scenarios are valid, but the absolute values needs further investigation.

Acknowledgments: The authors acknowledge the Erasmus Mundus program CoMEM (Coastal, Marine Engineering and Management) and the Lamminga Fund, for the scholarship during the development of this work.

Author Contributions: Bruno Primo led the project, performed all the Delft3D and Delft3D-WAQ modelling, did all the analysis and co-wrote the paper with Fernanda Achete. Sarith Mahanama performed all the downscaled river flow modelling, Marcus Thatcher and Mark Hemer provided the dynamically downscaled GCM output, Sutat Weesakui and Trang Duong collated and provided the field data required for model validation.

Conflicts of Interest: The authors declare no conflict of interest.

References

1. Bruun, P., Gerritsen, F. Stability of Coastal Inlets. *North-Holland Publishing Co*., Amsterdam, 1960, 123 pp.
2. Kjerfve, B., Coastal Lagoon Processes. *Elsevier Science Publishers*, Amsterdam, 1994, 577pp.
3. Barnes, H. Coastal lagoons, *Cambridge University Press*. 1980 106pp.
4. FitzGerald, D.M., Fenster, M.S., Argow, B.A., Buynevich, I.V. Coastal impacts due to sea-level rise. *Annu. Rev. Earth Planet Sci.* 2008, *36*, 601–647.
5. Anthony, A., J. Atwood, P. August, C. Byron, S. Cobb, C. Foster, C. Fry, A. Gold, K. Hagos, L. Heffner, D. Q. Kellogg, K. Lellis-Dibble, J. J. Opaluch, C. Oviatt, A. Pfeiffer-Herbert, N. Rohr, L. Smith, T. Smythe, J. Swift, and N. Vinhateiro. Coastal lagoons and climate change: ecological and social ramifications in U.S. Atlantic and Gulf coast ecosystems. *Ecology and Society*, 2009 14(1): 8.
6. Kjerfve, B. and Magill, K.E., Geographic and hydrodynamic characteristics of shallow coastal lagoons. *Marine Geology*, 1989 88, 187-199
7. Nichols, M.M., and Allen, G., Sedimentary processes in coastal lagoons. *Coastal lagoon research, present and future.* 1981, pp. 77-187
8. Haines, P. Anticipated Response of Coastal Lagoons to Sea Level Rise. IPWEA National Conference August 2008
9. Lesser, G., An Approach to Medium-term Coastal Morphological Modeling, PhD thesis, UNESCO-IHE/Delft University of Technology, 2009 (ISBN 978-0-415-55668-2).
10. DeVriend, H.J., Zyserman, J., Nicholson, J., Roelvink, J.A., Pechon, P., Southgate, H.N., Medium term 2DH coastal area modelling. *Coast. Eng*. 1993 21, 193–224.
11. Dabees, M., Kamphuis, J.W., ONELINE: efficient modeling of 3-D beach change. Proceedings of the 27th International Conference on Coastal Engineering, Sydney, Australia, ASCE, 2000 pp. 2700–2713
12. Hanson, H., Aarninkhof, S., Capobianco, M., Jimenez, J.A., Larson, M., Nicholls, R., Plant, N., Southgate, H.N., Steetzel, H.J., Stive, M.J.F., De Vriend, H.J., 2003. Modelling coastal evolution on early to decadal time scales. J. Coast. Res. 19 (4), 790–811.
13. Roelvink, J.A., Coastal morphodynamic evolution techniques. *Coast. Eng*. 2006, 53, 277–287.
14. Ranasinghe, R., Assessing Climate change impacts on Coasts: A Review. *Earth Science Reviews*, 2016, 160, 320-332.
15. Duong T., Ranasinghe R., Thatcher M., Mahanama S., Wang Z., Dissanayake P., Hemer M., Luijendijk A., Bamunawala J., Roelvink D. and Walstra D. 2018. Assessing climate change impacts on the stability of small tidal inlets: Part 2 – data rich environments. Marine Geology, Vol 395, 65-81
16. McGregor J, C-CAM: Geometric aspects and dynamical formulation. *CSIRO Marine and Atmospheric Research Tech Paper* 2005a, 70, 43 pp.
17. McGregor J and Dix M. An updated description of the conformal cubic atmospheric model. High resolution Simulation of the Atmosphere and Ocean. *K. Hamilton and W. Ohfuchi, Eds*. 2008, Springer, 51-76.
18. Schmidt F., Variable fine mesh in spectral global models. *Beitr. Phys. Atmos*. 1977, 50, 211-217.
19. Rotstayn L., A physically based scheme for the treatment of stratiform clouds and precipitation in large scale models. I: Description and evaluation of the microphysical processes. *Quart. J. Roy. Meteor. Soc*., 1997, 123, 1227-1282.
20. McGregor, J. L. A new convection scheme using a simple closure. In *Current issues in the parameterization of convection*, BMRC Research Report, 2003, 93, 33–36.
21. Kowalczyk E.; Garratt J.; Krummel P. Implementation of a soil-canopy scheme into the CSIRO GCM – Regional aspects of the model response. *CSIRO Martine and Atmospheric Research Tech Report*, 1994, 32, 65 pp.

22. McGregor, J. L.; Gordon H. B.; Watterson, I. G.; Dix, M. R; Rotstayn, L. D., The CSIRO 9-level atmospheric general circulation model. *CSIRO Div. Atmospheric Research Tech*. 1993, Paper No. 26, 89 pp.
23. Holtslag A and Boville B, Local versus non-local boundary layer diffusion in a global climate model. *J. Climate*, 1993, 6, 1825-1842.
24. Smith R, A scheme for predicting layer clouds and their water content in a General Circulation Model. *Quart. J. Roy. Meteor. Soc.* 1990, 116, 435-460.
25. Chouinard C, Beland M and McFarlane N, A simple gravity wave drag parameterization for use in medium-range weather forecast models. *Atmos-Ocean*, 1986, 24, 91-110.
26. Lacis A and Hansen J, A parameterisation of the absorption of solar radiation in the Earth's atmosphere. *J. Atmos. Sci*, 1974 31, 118-133.
27. Schwarzkopf, M.; Fels, S. The simplified exchange method revisited: An accurate, rapid method for computation of infrared cooling rates and fluxes. *J. Geophys. Res*. 1991, 96, 9075-9096.
28. Wang Y, Leung L, McGregor J, Lee D, Wang W, Ding Y and Kimura F, Regional climate modeling: Progress, challenges and prospects. *J. Meteor. Soc. Japan*. 2004, 82, 1599-1628.
29. Koster, R.D., Suarez, M.J., Ducharne, A., Stieglitz, M., Kumar, P., A catchment-based approach to modeling land surface processes in a general circulation model: 1. Model structure. *J. Geophys. Res*. 2000, 105 (20), 24,809–24,822.
30. Ducharne, A., R.D. Koster, M.J. Suarez, M. Stieglitz, and P. Kumar. A catchment-based approach to modeling land surface processes in a GCM. Part 2: Parameter estimation and model demonstration. *Journal of Geophysical Research Atmospheres*, 2000, 105(D20): 24823-24838.
31. Mahanama, P.P. Sarith & D. Koster, Randal & H. Reichle, Rolf & Zubair, Lareef. The role of soil moisture initialization in subseasonal and seasonal streamflow prediction – A case study in Sri Lanka. *Advances in Water Resources*. 2008, 31. 1333-1343. 10.1016
32. Lesser, G., Roelvink, J.A., Van Kester, J.A.T.M., Stelling, G.S., Development and validation of a three-dimensional morphological model. *Coast. Eng*. 2004, 51, 883–915.
33. Pornpinatepong, S.; Tanaka, H.; Takasaki, M. Application of 2-D Vertically Averaged Boundary-Fitted Coordinate Model of Tidal Circulation in Thale Sap Songkhla, Thailand. *Walailak J Sci & Tech* 2006 3(1): 105-118
34. Viet, N. T., Tanaka, H., Takasaki, M. and Yamaji, H. In-situ investigation and simulation of water quality changes in Songkhla Lake, Thailand. Proceedings of the 4th Asian and Pacific Coasts Vol. 4., 2007 Nanjing, China.
35. Aubrey, D. G.; McSherry, T. R., and Eliet, P.P., Effects of multiple inlet morphology on tidal exchange: Waquoit Bay, Massachussettes. In: Aubrey, D. G. and Giese, G. S. (eds.), Formation and Evolution of Multiple Tidal Inlets. Washington, D.C., *American Geophysical Union*, 1993 pp. 231-235.